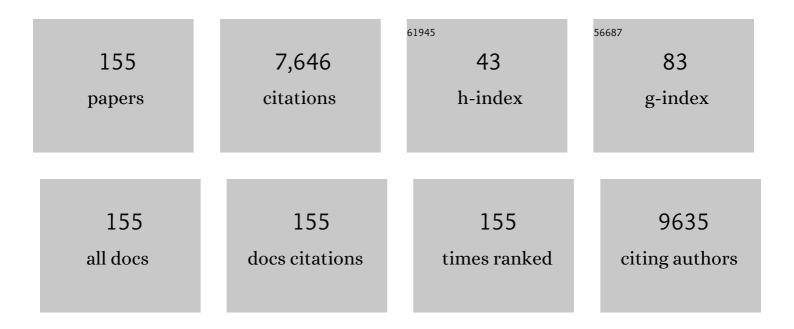
Weichang Hao

List of Publications by Year in descending order

Source: https://exaly.com/author-pdf/3160392/publications.pdf Version: 2024-02-01



#	Article	IF	CITATIONS
1	Epitaxial growth of bilayer Bi(110) on two-dimensional ferromagnetic Fe ₃ GeTe ₂ . Journal of Physics Condensed Matter, 2022, 34, 074003.	0.7	5
2	First-principles study on the electronic structures and diffusion behaviors of intrinsic defects in BiOCl. Computational Materials Science, 2022, 203, 111088.	1.4	6
3	Large-Gap Quantum Spin Hall State and Temperature-Induced Lifshitz Transition in Bi ₄ Br ₄ . ACS Nano, 2022, 16, 3036-3044.	7.3	17
4	Metal cocatalyst mediated photocatalytic dehydrogenative-condensation and direct condensation cross-coupling of aniline and alcohol. Applied Catalysis B: Environmental, 2022, 309, 121264.	10.8	14
5	Roles of Cocatalysts on BiVO ₄ Photoanodes for Photoelectrochemical Water Oxidation: A Minireview. Energy & Fuels, 2022, 36, 11394-11403.	2.5	14
6	Boosting Lightâ€Driven Photocatalytic Water Splitting of Bi ₄ NbO ₈ Br by Polarization Field. Solar Rrl, 2022, 6, .	3.1	4
7	Facet-dependent Electronic Quantum Diffusion in the High-Order Topological Insulator <mml:math xmlns:mml="http://www.w3.org/1998/Math/MathML" display="inline" overflow="scroll"><mml:msub><mml:mi>Bi</mml:mi><mml:mn>4</mml:mn></mml:msub><mml:msub><mml:mi Physical Review Applied, 2022, 17.</mml:mi </mml:msub></mml:math 	>ðr <td>:mi><mmla< td=""></mmla<></td>	:mi> <mmla< td=""></mmla<>
8	A novel Cl- modification approach to develop highly efficient photocatalytic oxygen evolution over BiVO4 with AQE of 34.6%. Nano Energy, 2021, 81, 105651.	8.2	43
9	Theoretical insights into nitrogen oxide activation on halogen defect-rich {001} facets of bismuth oxyhalide. Journal of Materials Science and Technology, 2021, 77, 217-222.	5.6	6
10	Moiréâ€Potentialâ€Induced Band Structure Engineering in Graphene and Silicene. Small, 2021, 17, e1903769.	5.2	9
11	Synthesis of magnetic core–shell iron nanochains for potential applications in Cr(VI) ion pollution treatment. Rare Metals, 2021, 40, 176-179.	3.6	9
12	Tuning the performance of nitrogen reduction reaction by balancing the reactivity of N2 and the desorption of NH3. Nano Research, 2021, 14, 4093-4099.	5.8	27
13	Ureaâ€Assisted Synthesis and Tailoring Cobalt Cores for Synergetic Promotion of Hydrogen Evolution Reaction in Acid and Alkaline Media. Advanced Energy and Sustainability Research, 2021, 2, 2000091.	2.8	5
14	The Synergistic Effect of Heteroatom Doping and Vacancy on The Reduction of CO ₂ by Photocatalysts. ChemNanoMat, 2021, 7, 894-901.	1.5	6
15	Germanene Nanosheets: Achieving Superior Sodiumâ€ion Storage via Pseudointercalation Reactions. Small Structures, 2021, 2, 2100041.	6.9	20
16	Kondo Holes in the Two-Dimensional Itinerant Ising Ferromagnet Fe ₃ GeTe ₂ . Nano Letters, 2021, 21, 6117-6123.	4.5	23
17	Epitaxial Growth of Quasi-One-Dimensional Bismuth-Halide Chains with Atomically Sharp Topological Non-Trivial Edge States. ACS Nano, 2021, 15, 14850-14857.	7.3	12

Recent Progress on 2D Kagome Magnets: Binary T<i>_m</i>Sn<i>_n</i>(T = Fe,) Tj ETQq0 0.0 rgBT /Overlock 10

#	Article	IF	CITATIONS
19	Unveiling the activity origin of ultrathin BiOCl nanosheets for photocatalytic CO2 reduction. Applied Catalysis B: Environmental, 2021, 299, 120679.	10.8	77
20	Enhancing the macroscopic polarization of CdS for piezo-photocatalytic water splitting. Nano Energy, 2021, 90, 106635.	8.2	77
21	Sulfurized Polyacrylonitrile as a High-Performance and Low-Volume Change Anode for Robust Potassium Storage. ACS Nano, 2021, 15, 18419-18428.	7.3	17
22	Electric-Field-Driven Negative Differential Conductance in 2D van der Waals Ferromagnet Fe ₃ GeTe ₂ . Nano Letters, 2021, 21, 9233-9239.	4.5	10
23	Promoted Photocharge Separation in 2D Lateral Epitaxial Heterostructure for Visibleâ€Lightâ€Driven CO ₂ Photoreduction. Advanced Materials, 2020, 32, e2004311.	11.1	74
24	Effect of Pd and Au on Hydrogen Abstraction and C–C Cleavage in Photoconversion of Glycerol: Beyond Charge Separation. Journal of Physical Chemistry C, 2020, 124, 20320-20327.	1.5	6
25	Materializing efficient methanol oxidation via electron delocalization in nickel hydroxide nanoribbon. Nature Communications, 2020, 11, 4647.	5.8	117
26	Hydrogen Terminated Germanene for a Robust Selfâ€Powered Flexible Photoelectrochemical Photodetector. Small, 2020, 16, e2000283.	5.2	58
27	Supercritical CO ₂ -constructed intralayer [Bi ₂ O ₂] ²⁺ structural distortion for enhanced CO ₂ electroreduction. Journal of Materials Chemistry A, 2020, 8, 13320-13327.	5.2	29
28	Controlled hydrogenation into defective interlayer bismuth oxychloride via vacancy engineering. Communications Chemistry, 2020, 3, .	2.0	22
29	Palladium forms Ohmic contact on hydrogen-terminated diamond down to 4 K. Applied Physics Letters, 2020, 116, .	1.5	14
30	Efficient Ammonia Electrosynthesis from Nitrate on Strained Ruthenium Nanoclusters. Journal of the American Chemical Society, 2020, 142, 7036-7046.	6.6	542
31	In-situ grafting of N-doped carbon nanotubes with Ni encapsulation onto MOF-derived hierarchical hybrids for efficient electrocatalytic hydrogen evolution. Carbon, 2020, 163, 178-185.	5.4	56
32	Memristive devices based on 2D-BiOI nanosheets and their applications to neuromorphic computing. Applied Physics Letters, 2020, 116, .	1.5	13
33	Reversible Potassium Intercalation in Blue Phosphorene–Au Network Driven by an Electric Field. Journal of Physical Chemistry Letters, 2020, 11, 5584-5590.	2.1	5
34	Nanomagnetism variation with fluorine content in Co(OH)F. Journal of Alloys and Compounds, 2020, 825, 153916.	2.8	5
35	Two-Dimensional Van der Waals Heterostructures for Synergistically Improved Surface-Enhanced Raman Spectroscopy. ACS Applied Materials & Interfaces, 2020, 12, 21985-21991.	4.0	17
36	The role of oxygen vacancies in the high cycling endurance and quantum conductance in BiVO ₄ â€based resistive switching memory. InformaÄnÃ-Materiály, 2020, 2, 960-967.	8.5	21

#	Article	IF	CITATIONS
37	BiOBr nanoflakes with strong Kerr nonlinearity towards hybrid integrated photonic devices. , 2020, , .		1
38	Direct Observation of Oxygen Vacancy Selfâ€Healing on TiO ₂ Photocatalysts for Solar Water Splitting. Angewandte Chemie, 2019, 131, 14367-14371.	1.6	24
39	Direct Observation of Oxygen Vacancy Selfâ€Healing on TiO ₂ Photocatalysts for Solar Water Splitting. Angewandte Chemie - International Edition, 2019, 58, 14229-14233.	7.2	138
40	Evidence for the dynamic relaxation behavior of oxygen vacancies in Aurivillius Bi2MoO6 from dielectric spectroscopy during resistance switching. Journal of Materials Chemistry C, 2019, 7, 8915-8922.	2.7	10
41	A Boolean OR gate implemented with an optoelectronic switching memristor. Applied Physics Letters, 2019, 115, .	1.5	20
42	Highly nonlinear BiOBr nanoflakes for hybrid integrated photonics. APL Photonics, 2019, 4, .	3.0	31
43	Hierarchical Nanoassembly of MoS ₂ /Co ₉ S ₈ /Ni ₃ S ₂ /Ni as a Highly Efficient Electrocatalyst for Overall Water Splitting in a Wide pH Range. Journal of the American Chemical Society. 2019, 141, 10417-10430.	6.6	653
44	Boosting NIR-driven photocatalytic water splitting by constructing 2D/3D epitaxial heterostructures. Journal of Materials Chemistry A, 2019, 7, 13629-13634.	5.2	30
45	Realization of Strained Stanene by Interface Engineering. Journal of Physical Chemistry Letters, 2019, 10, 1558-1565.	2.1	25
46	Two dimensional bismuth-based layered materials for energy-related applications. Energy Storage Materials, 2019, 19, 446-463.	9.5	89
47	Recent Progress on Twoâ€Dimensional Heterostructures for Catalytic, Optoelectronic, and Energy Applications. ChemElectroChem, 2019, 6, 2841-2851.	1.7	18
48	Photoelectrochemical properties of BiVO4 thin films with NaOH chemical treatment. Rare Metals, 2019, 38, 446-452.	3.6	4
49	A non-enzymatic photoelectrochemical glucose sensor based on BiVO4 electrode under visible light. Sensors and Actuators B: Chemical, 2019, 291, 34-41.	4.0	67
50	2D Heterostructures: Monolayer Epitaxial Heterostructures for Selective Visibleâ€Lightâ€Driven Photocatalytic NO Oxidation (Adv. Funct. Mater. 15/2019). Advanced Functional Materials, 2019, 29, 1970100.	7.8	1
51	Role of Charge Density Wave in Monatomic Assembly in Transition Metal Dichalcogenides. Advanced Functional Materials, 2019, 29, 1900367.	7.8	28
52	High Pressure Driven Isostructural Electronic Phase Separation in 2D BiOI. Physica Status Solidi - Rapid Research Letters, 2019, 13, .	1.2	2
53	Solid Base Bi ₂₄ O ₃₁ Br ₁₀ (OH) _δ with Active Lattice Oxygen for the Efficient Photoâ€Oxidation of Primary Alcohols to Aldehydes. Angewandte Chemie - International Edition, 2019, 58, 6265-6270.	7.2	78
54	Solid Base Bi ₂₄ O ₃₁ Br ₁₀ (OH) _δ with Active Lattice Oxygen for the Efficient Photoâ€Oxidation of Primary Alcohols to Aldehydes. Angewandte Chemie, 2019, 131, 6331-6336.	1.6	11

Weichang Hao

#	Article	IF	CITATIONS
55	Promoting photoreduction properties via synergetic utilization between plasmonic effect and highly active facet of BiOCl. Nano Energy, 2019, 57, 398-404.	8.2	52
56	Monolayer Epitaxial Heterostructures for Selective Visible‣ightâ€Driven Photocatalytic NO Oxidation. Advanced Functional Materials, 2019, 29, 1808084.	7.8	76
57	Boosting Visible-Light-Driven Photo-oxidation of BiOCl by Promoted Charge Separation via Vacancy Engineering. ACS Sustainable Chemistry and Engineering, 2019, 7, 3010-3017.	3.2	101
58	Enhancement of photocatalytic activity of Bi2MoO6 by fluorine substitution. Applied Surface Science, 2019, 467-468, 740-748.	3.1	36
59	Selective Ferroelectric BiOI/Bi ₄ Ti ₃ O ₁₂ Heterostructures for Visible Light-Driven Photocatalysis. Journal of Physical Chemistry C, 2019, 123, 517-525. Giant zero-field cooling exchange-bias-like behavior in antiperovskite <mml:math< td=""><td>1.5</td><td>36</td></mml:math<>	1.5	36
60	xmlns:mml="http://www.w3.org/1998/Math/MathML"> < mml:mrow> < mml:mi mathvariant="normal">M < /mml:mi> < mml:msub> < mml:mi mathvariant="normal">n < /mml:mi> < mml:mn> 3 < /mml:mn> < /mml:msub> < mml:mi mathvariant="normal">C < /mml:mi> < mml:msub> < mml:mi	0.9	3
61	mathvariant="normal">o <mml:mrow><mml:mn>0.61</mml:mn></mml:mrow> <mml:mi s-p orbital hybridization: a strategy for developing efficient photocatalysts with high carrier mobility. Science Bulletin, 2018, 63, 465-468.</mml:mi 	4.3	37
62	Activating Titania for Efficient Electrocatalysis by Vacancy Engineering. ACS Catalysis, 2018, 8, 4288-4293.	5.5	141
63	Quantum Monte Carlo study of hard-core bosons in Creutz ladder with zero flux. Chinese Physics B, 2018, 27, 010204.	0.7	1
64	Band-gap engineering of BiOCl with oxygen vacancies for efficient photooxidation properties under visible-light irradiation. Journal of Materials Chemistry A, 2018, 6, 2193-2199.	5.2	232
65	Metal@semiconductor core-shell nanocrystals with atomically organized interfaces for efficient hot electron-mediated photocatalysis. Nano Energy, 2018, 48, 44-52.	8.2	118
66	Realization of flat band with possible nontrivial topology in electronic Kagome lattice. Science Advances, 2018, 4, eaau4511.	4.7	131
67	Photocatalytic Reduction on Bismuth-Based <i>p</i> Block Semiconductors. ACS Sustainable Chemistry and Engineering, 2018, 6, 15936-15953.	3.2	62
68	Electronic Band Engineering in Elemental 2D Materials. Advanced Materials Interfaces, 2018, 5, 1800749.	1.9	16
69	Dirac Signature in Germanene on Semiconducting Substrate. Advanced Science, 2018, 5, 1800207.	5.6	59
70	Enhanced Photocatalytic Activity of Bi 24 O 31 Br 10 : Constructing Heterojunction with BiOI. Journal of Materials Science and Technology, 2017, 33, 281-284.	5.6	31
71	Oxygen-Impurity-Induced Direct–Indirect Band Gap in Perovskite SrTaO ₂ N. Journal of Physical Chemistry C, 2017, 121, 6864-6867.	1.5	14
72	Rectifying Characteristics and Semiconductor–Metal Transition Induced by Interfacial Potential in the Mn3CuN/n-Si Intermetallic Heterojunction. ACS Applied Materials & Interfaces, 2017, 9, 12592-12600.	4.0	2

#	Article	IF	CITATIONS
73	Shape-Controlled Metal-Free Catalysts: Facet-Sensitive Catalytic Activity Induced by the Arrangement Pattern of Noncovalent Supramolecular Chains. ACS Nano, 2017, 11, 4866-4876.	7.3	31
74	The origin of enhanced photocatalytic activities of hydrogenated TiO ₂ nanoparticles. Dalton Transactions, 2017, 46, 10694-10699.	1.6	24
75	Construction of 2D lateral pseudoheterostructures by strain engineering. 2D Materials, 2017, 4, 025102.	2.0	31
76	O ₃ fast and simple treatment-enhanced p-doped in Spiro-MeOTAD for CH ₃ NH ₃ I vapor-assisted processed CH ₃ NH ₃ PbI ₃ perovskite solar cells. Chinese Physics B, 2017, 26, 068803.	0.7	5
77	Efficient visible-light photocatalysts by constructing dispersive energy band with anisotropic p and s-p hybridization states. Current Opinion in Green and Sustainable Chemistry, 2017, 6, 93-100.	3.2	28
78	Silicene: A Promising Anode for Lithiumâ€lon Batteries. Advanced Materials, 2017, 29, 1606716.	11.1	179
79	Liquid-Phase Exfoliation into Monolayered BiOBr Nanosheets for Photocatalytic Oxidation and Reduction. ACS Sustainable Chemistry and Engineering, 2017, 5, 10499-10508.	3.2	140
80	Enhancement of charge separation in ferroelectric heterogeneous photocatalyst Bi ₄ (SiO ₄) ₃ /Bi ₂ SiO ₅ nanostructures. Dalton Transactions, 2017, 46, 15582-15588.	1.6	25
81	A specific mapping between topological superconductors and topological insulators. Europhysics Letters, 2017, 118, 61002.	0.7	0
82	Threeâ€Ðimensional Hierarchical Architectures Derived from Surfaceâ€Mounted Metal–Organic Framework Membranes for Enhanced Electrocatalysis. Angewandte Chemie - International Edition, 2017, 56, 13781-13785.	7.2	193
83	Topological superconductors from one-dimensional periodically modulated Majorana chains. Scientific Reports, 2017, 7, 9210.	1.6	5
84	Single-unit-cell layer established Bi2WO6 3D hierarchical architectures: Efficient adsorption, photocatalysis and dye-sensitized photoelectrochemical performance. Applied Catalysis B: Environmental, 2017, 219, 526-537.	10.8	264
85	Enhanced energy transfer in heterogeneous nanocrystals for near infrared upconversion photocurrent generation. Nanoscale, 2017, 9, 18661-18667.	2.8	14
86	Threeâ€Dimensional Hierarchical Architectures Derived from Surfaceâ€Mounted Metal–Organic Framework Membranes for Enhanced Electrocatalysis. Angewandte Chemie, 2017, 129, 13969-13973.	1.6	42
87	Structurally Wellâ€Defined Au@Cu _{2â^'} <i>_x</i> S Core–Shell Nanocrystals for Improved Cancer Treatment Based on Enhanced Photothermal Efficiency. Advanced Materials, 2016, 28, 3094-3101.	11.1	228
88	Indirect-Direct Band Transformation of Few-Layer BiOCl under Biaxial Strain. Journal of Physical Chemistry C, 2016, 120, 8589-8594.	1.5	29
89	A ferroelectric photocatalyst Ag ₁₀ Si ₄ O ₁₃ with visible-light photooxidation properties. Journal of Materials Chemistry A, 2016, 4, 10992-10999.	5.2	46
90	Magnetic field actuated manipulation and transfer of oil droplets on a stable underwater superoleophobic surface. Physical Chemistry Chemical Physics, 2016, 18, 16202-16207.	1.3	20

#	Article	IF	CITATIONS
91	Metal–silicene interaction studied by scanning tunneling microscopy. Journal of Physics Condensed Matter, 2016, 28, 034002.	0.7	9
92	Manipulating coupling state and magnetism of Mn-doped ZnO nanocrystals by changing the coordination environment of Mn via hydrogen annealing. Chinese Physics B, 2016, 25, 017301.	0.7	4
93	From Cu2S nanocrystals to Cu doped CdS nanocrystals through cation exchange: controlled synthesis, optical properties and their p-type conductivity research. Science China Materials, 2015, 58, 693-703.	3.5	23
94	Investigation of electron-phonon coupling in epitaxial silicene by <i>in situ</i> Raman spectroscopy. Physical Review B, 2015, 91, .	1.1	67
95	Modulation of Photocatalytic Properties by Strain in 2D BiOBr Nanosheets. ACS Applied Materials & Interfaces, 2015, 7, 27592-27596.	4.0	130
96	Nonmetal P-doped hematite photoanode with enhanced electron mobility and high water oxidation activity. Energy and Environmental Science, 2015, 8, 1231-1236.	15.6	202
97	Visible-Light Photocatalytic Activity of S-Doped α-Bi ₂ O ₃ . Journal of Physical Chemistry C, 2015, 119, 14094-14101.	1.5	56
98	Heterovalentâ€Dopingâ€Enabled Efficient Dopant Luminescence and Controllable Electronic Impurity Via a New Strategy of Preparing Ilâ^'VI Nanocrystals. Advanced Materials, 2015, 27, 2753-2761.	11.1	67
99	Enhanced photocatalysis activity of ferroelectric KNbO ₃ nanofibers compared with antiferroelectric NaNbO ₃ nanofibers synthesized by electrospinning. RSC Advances, 2015, 5, 72410-72415.	1.7	30
100	Aligned ZnO:Co nanorod arrays: Electrophoretic deposition fabrication and magnetic manipulation. Ceramics International, 2015, 41, 3456-3460.	2.3	10
101	Plasmonic Photocatalytic Activity of Silver Nano-Particles Using Carbon Sphere as Support. Energy and Environment Focus, 2015, 4, 128-132.	0.3	3
102	Enhancing visible-light photocatalytic activity of α-Bi 2 O 3 via non-metal N and S doping. Chinese Physics B, 2014, 23, 038103.	0.7	11
103	Variation of the coordination environment and its effect on the white light emission properties in a Mn-doped ZnO–ZnS complex structure. Physical Chemistry Chemical Physics, 2014, 16, 4544.	1.3	12
104	Biocompatibility of TiO2 and TiO2/heparin coatings on NiTi alloy. Applied Surface Science, 2014, 313, 172-182.	3.1	18
105	Bismuth Oxybromide with Reasonable Photocatalytic Reduction Activity under Visible Light. ACS Catalysis, 2014, 4, 954-961.	5.5	300
106	Visible Light Photocatalytic Properties of Metastable γ-Bi2O3 with Different Morphologies. Journal of Materials Science and Technology, 2014, 30, 192-196.	5.6	59
107	A dye-sensitized visible light photocatalyst-Bi24O31Cl10. Scientific Reports, 2014, 4, 7384.	1.6	91
108	Silver microgrid transparent conductive electrode based on bulk plasmon effect for ultraviolet wavelength application. Physica Status Solidi - Rapid Research Letters, 2013, 7, 1071-1075.	1.2	5

#	Article	IF	CITATIONS
109	The variation of Mn-dopant distribution state with x and its effect on the magnetic coupling mechanism in Zn 1â°' x Mn x O nanocrystals. Chinese Physics B, 2013, 22, 107501.	0.7	4
110	Manipulation of domain wall mobility by oxygen vacancy ordering in multiferroic YMnO3. Physical Chemistry Chemical Physics, 2013, 15, 20010.	1.3	32
111	Fabrication and UV-sensing properties of one-dimensional β-Ga ₂ O ₃ nanomaterials. Physica Status Solidi (A) Applications and Materials Science, 2013, 210, 1861-1865.	0.8	15
112	Nanostructured Magnetic Materials. Journal of Nanomaterials, 2013, 2013, 1-2.	1.5	1
113	Biocompatibility of Nanoporous TiO2Coating on NiTi Alloy Prepared via Dealloying Method. Journal of Nanomaterials, 2012, 2012, 1-7.	1.5	4
114	Improving the Solubility of Mn and Suppressing the Oxygen Vacancy Density in Zn _{0.98} Mn _{0.02} O Nanocrystals via Octylamine Treatment. ACS Applied Materials & Interfaces, 2012, 4, 4470-4475.	4.0	18
115	Magnetic properties and microstructures of iron oxide@mesoporous silica core-shell composite for applications in magnetic dye separation. Journal of Applied Physics, 2012, 111, 07B301.	1.1	10
116	Controllable synthesis and magnetic investigation of ZnO: Co nanowires and nanotubes. Materials Letters, 2012, 87, 101-104.	1.3	11
117	Graphene covered SiC powder as advanced photocatalytic material. Applied Physics Letters, 2012, 100, 023113.	1.5	65
118	Effect of Cu Co-doping on the magnetism of Zn0.95Co0.05O films. Journal of Shanghai Jiaotong University (Science), 2012, 17, 738-742.	0.5	1
119	Effect of Intrinsic Oxygen Vacancy on the Electronic Structure of γ-Bi ₂ O ₃ : First-Principles Calculations. Journal of Physical Chemistry C, 2012, 116, 1251-1255.	1.5	44
120	Controllable synthesis of Zn0.95Co0.05O nanowires and nanotubes by electrophoretic deposition method. Transactions of Nonferrous Metals Society of China, 2012, 22, s95-s99.	1.7	5
121	Al Doped ZnO Nanogranular Film Fabricated by Layer-By-Layer Self-Assembly Method and Its Application for Gas Sensors. Journal of Nanoscience and Nanotechnology, 2011, 11, 10649-10653.	0.9	5
122	BiOCl nano/microstructures on substrates: Synthesis and photocatalytic properties. Materials Letters, 2011, 65, 1344-1347.	1.3	64
123	Enhancement of magnetism of Zn0.95Co0.05O films by p-type Cu+ doping. Progress in Natural Science: Materials International, 2011, 21, 31-35.	1.8	3
124	First-principles calculations of novel sillenite compounds Bi24M2O40 (M=Se or Te). Rare Metals, 2011, 30, 135-139.	3.6	8
125	Visible-light photocatalytic properties of γ-Bi2O3 composited with Fe2O3. Rare Metals, 2011, 30, 140-143.	3.6	6
126	A Transition Phase in the Transformation from α-, β- and â^Š- to δ-Bismuth Oxide. Chinese Physics Letters, 2011, 28, 056101.	1.3	20

Weichang Hao

#	Article	IF	CITATIONS
127	Bio-Inducing Growth of ZnO Hollow Spheres in Lotus Root. Journal of Nanoscience and Nanotechnology, 2010, 10, 7439-7442.	0.9	Ο
128	Positron annihilation study of structural effect on photocatalytic activity of mesoporous TiO2 thin films. Nuclear Instruments & Methods in Physics Research B, 2010, 268, 2362-2365.	0.6	5
129	LUMINESCENT PROPERTY OF ZNO GRANULAR FILMS WITH DIFFERENT PARTICLE SIZE. International Journal of Modern Physics B, 2010, 24, 2827-2832.	1.0	2
130	Al doped ZnO nanogranular film fabricated by LBL method and its application for gas sensors. , 2010, , .		1
131	Comparison Study of Corrosion Behavior and Biocompatibility of Polyethyleneimine (PEI)/Heparin and Chitosan/Heparin Coatings on NiTi alloy. Journal of Materials Science and Technology, 2010, 26, 1027-1031.	5.6	31
132	Evidence of Surface-Preferential Co Distribution in ZnO Nanocrystal and Its Effects on the Ferromagnetic Property. ACS Applied Materials & amp; Interfaces, 2010, 2, 2053-2059.	4.0	17
133	Variation of structural and magnetic properties with Co-doping in Zn1â^'xCoxO nanocrystals. Journal of Applied Physics, 2009, 105, .	1.1	24
134	Synthesis of large-sized monodisperse polystyrene microspheres by dispersion polymerization with dropwise monomer feeding procedure. Colloid and Polymer Science, 2009, 287, 243-248.	1.0	24
135	Enhancement of ferromagnetism in Zn0.95Co0.05O films by lithium codoping. Journal of Applied Physics, 2009, 106, .	1.1	6
136	Employment of a metal microgrid as a front electrode in a sandwich-structured photodetector. Applied Optics, 2009, 48, 3638.	2.1	3
137	Growth Mechanism for ZnO Nanorod Array in a Metastable Supersaturation Solution. Journal of Nanoscience and Nanotechnology, 2009, 9, 909-913.	0.9	5
138	Fabrication and biocompatibility of polyethyleneimine/heparin self-assembly coating on NiTi alloy. Thin Solid Films, 2008, 516, 5168-5171.	0.8	22
139	Effect of crystallization quality on ferromagnetism in Zn1â^'xCoxO nanopowders. Materials Letters, 2008, 62, 403-406.	1.3	16
140	Photocatalytic properties of BiOX (X = Cl, Br, and I). Rare Metals, 2008, 27, 243-250.	3.6	297
141	A simple and green approach for preparation of ZnO2 and ZnO under sunlight irradiation. Chemical Physics Letters, 2007, 443, 342-346.	1.2	73
142	Luminescence of nanosized ZnO/polyaniline films prepared by self-assembly. Ceramics International, 2007, 33, 785-788.	2.3	15
143	Luminescent properties of ZnO sol and film doped with Tb3+ ion. Materials Science & Engineering A: Structural Materials: Properties, Microstructure and Processing, 2006, 425, 346-348.	2.6	17
144	Effect of MgO doping on the luminescent properties of ZnO. Materials Science and Engineering B: Solid-State Materials for Advanced Technology, 2006, 129, 93-95.	1.7	15

#	Article	IF	CITATIONS
145	Blue-emitting ZnO sol and film obtained by sol-gel process. Journal of Sol-Gel Science and Technology, 2006, 39, 37-39.	1.1	20
146	Photocatalytic activity TiO2 granular films prepared by layer-by-layer self-assembly method. Journal of Materials Science, 2005, 40, 1251-1253.	1.7	8
147	Effects of heat treatment on properties of ITO films prepared by rf magnetron sputtering. Vacuum, 2004, 75, 183-188.	1.6	221
148	Light-storing photocatalyst. Applied Physics Letters, 2004, 85, 5778-5780.	1.5	34
149	Effects of heat treatment on properties of ITO films prepared by rf magnetron sputtering. Vacuum, 2004, 75, 183-183.	1.6	12
150	Photocatalytic activity studies of TiO2 thin films prepared by r.f. magnetron reactive sputtering. Vacuum, 2003, 72, 79-84.	1.6	29
151	Preparation and characterization of a new long afterglow indigo phosphor Ca12Al14O33:Nd,Eu. Materials Letters, 2003, 57, 4315-4318.	1.3	57
152	Studies on photocatalytic activity and transmittance spectra of TiO2 thin films prepared by r.f. magnetron sputtering method. Surface and Coatings Technology, 2002, 155, 141-145.	2.2	94
153	Improvement of photocatalytic activity of TiO2 thin film by Sn ion implantation. Vacuum, 2002, 65, 155-159.	1.6	63
154	Comparison of the photocatalytic activity of TiO2 powder with different particle size. Journal of Materials Science Letters, 2002, 21, 1627-1629.	0.5	39
155	Raman Studies on Silicene and Germanene. Surface Innovations, 0, , 1-31.	1.4	2